# Return of the EMC effect: Finite nuclei

Jason R. Smith and Gerald A. Miller
*Department of Physics, University of Washington, Seattle, Washington 98195-1560*
(Received 6 February 2002; published 13 May 2002)

A light front formalism for deep inelastic lepton scattering from finite nuclei is developed. In particular, the nucleon plus momentum distribution and a finite system analog of the Hugenholtz–van Hove theorem are presented. Using a relativistic mean field model, numerical results for the plus momentum distribution and ratio of bound to free nucleon structure functions for oxygen, calcium, and lead are given. We show that we can incorporate light front physics with excellent accuracy while using easily computed equal time wave functions. Assuming nucleon structure is not modified in-medium we find that the calculations are not consistent with the binding effect apparent in the data not only in the magnitude of the effect, but also in the dependence on the number of nucleons.

DOI: 10.1103/PhysRevC.65.055206 PACS number(s): 25.30.Mr, 21.60.−n, 13.60.−r, 11.80.−m

## I. INTRODUCTION

The nuclear structure function $F_{2A}(x)$ is smaller than $A$ times the free nucleon structure function $AF_{2N}(x)$ for values of $x$ in the regime where valence quarks are dominant. This phenomenon, known as the European Muon Collaboration (EMC) effect [1], has been known for almost 20 years. Nevertheless, the significance of this observation remains unresolved even though there is a clear interpretation within the parton model: a valence quark in a bound nucleon carries less momentum than a valence quark in a free one. There are many possible explanations, but no universally accepted one. The underlying mechanism responsible for the transfer of momentum within the constituents of the nucleus has not yet been specified. One popular mechanism involves ordinary nuclear binding which, in its simplest form, is represented by evaluating the free nucleon structure function at a value of $x$ increased by a factor of the average separation energy divided by the nucleon mass $\overline{\epsilon}/M \simeq 0.04$. The validity of this binding effect has been questioned; see the reviews [2–5].

The Bjorken variable $x$ is a fraction of the plus component of momentum, and the desire to obtain a more precise evaluation and understanding of the binding effect lead us to attempt to obtain a nuclear wave function in which the momentum of the nucleons is expressed in terms of this same plus component. Therefore we applied light front dynamics to determine nuclear wave functions [6]. In this formalism one defines $x^{\pm} = x^0 \pm x^3$ and quantizes on equal $x^+$ surfaces that have a constant light front time, $\tau$. The conjugate operator $P^-$ acts as an evolution operator for $\tau$. The plus momentum is canonically conjugate to the spatial $x^-$ variable. This light front formalism has a variety of advantages [7–14] and also entails complications [15].

Our most recent result [16] is that the use of the relativistic mean field approximation, and the assumption that the structure of the nucleon is not modified by effects of the medium, to describe infinite nuclear matter leads to no appreciable binding effect. The failure was encapsulated in terms of the Hugenholtz–van Hove theorem [17] that states that the average nuclear binding energy per nucleon is equal to the binding energy of a nucleon at the top of the Fermi sea. The light front version of this theorem is obtained from the requirement that, in the nuclear rest frame, the expectation values of the total plus and minus momentum are equal. The original version of the theorem was obtained in a nonrelativistic theory in which nucleons are the only degrees of freedom. Here, the mesons are important and the theory is relativistic, but the theorem still holds. This theorem can be shown to restrict [16] the plus momentum carried by nucleons to be the mass of the nucleus, which in turn implies that the probability for a nucleon to have a plus momentum $k^+$ is narrowly peaked about $k^+ = M_A/A = \overline{M}$. Thus the only binding effect arises from the average binding energy, which is much smaller than the average separation energy. Therefore dynamics beyond the relativistic mean field approximation must be invoked to explain the EMC effect. This conclusion was limited to the case of infinite nuclear matter, and the computed nuclear structure function could only be compared with data on finite nuclear targets extrapolated to the limit $A \to \infty$. The goal of the present work is to extend the results to finite nuclei; the main complication arises from the spatial dependence of the nucleon and meson fields.

We briefly outline our procedure. In Secs. II and III we present the covariant deep inelastic scattering formalism of Ref. [18] and derive its representation in terms of nucleon single particle wave functions. The plus momentum distribution follows from this representation in Sec. IV where we also derive new version of the Hugenholtz–van Hove theorem. Then we present the results of analytic and numerical calculations in Sec. V, the latter giving an $A$ dependence of the ratio function contrary to experimental results. This again gives the result that the use of the relativistic mean field approximation, combined with the assumption that the nuclear medium does not modify the structure of the nucleon, cannot describe the EMC effect. The reasons for the subtle differences between the results for finite nuclei and nuclear matter are detailed in Sec. VI. Finally, we summarize and discuss possible implications.

## II. NUCLEON GREEN'S FUNCTION FOR FINITE NUCLEI

We begin with the covariant plus momentum distribution function

 

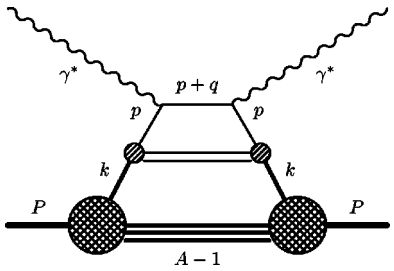


FIG. 1. Feynman diagram for deep inelastic scattering. A nucleus of momentum $P$ is struck by a virtual photon of momentum $q$. We label nucleon momentum $k$, and quark momentum $p$.

$$f_N(y)=\int \frac{d^4k}{(2\pi)^4}\,\delta\left(y-\frac{k^0+k^3}{\overline{M}}\right)\mathrm{Tr}[\gamma^+\chi^A(k,P)], \tag{2.1}$$

where we identify

$$\chi^A(k,P)\equiv -i\int d^4x\int d^4y e^{-ik\cdot(x-y)}G^C(x,y), \tag{2.2}$$

where $G^C(x,y)$ is the connected part of the nucleon Green's function

$$iG(x,y)\equiv\langle P|T^+\{\psi'(x)\overline{\psi}'(y)\}|P\rangle. \tag{2.3}$$

This result is directly determined from the Feynman diagram in Fig. 1 following Ref. [18], but with $\chi$ having a different normalization. So far this is independent of the particular relativistic mean field model, but for concreteness we use a quantum hadrodynamics (QHD) Lagrangian [19,20], specifically QHD-I as in Ref. [21], where the nucleon fields, $\psi'$ appearing in Eq. (2.3) are those appearing in the Lagrangian. Light front quantization requires that the plus component of all vector potential fields vanishes, and this is obtained by using the Soper-Yan transformation [22,23]

$$\psi'(x)\equiv e^{-ig_v\Lambda(x)}\psi(x),\quad \partial^+\Lambda(x)=V^+(x) \tag{2.4}$$

to define the nucleon field operator $\psi$ for various models [16]. This transformation allows the use of the eigenmode expansion for the $\psi$ fields obtained previously in Ref. [21]

$$\begin{aligned}\psi(x)&=\sum_\alpha\,[a_\alpha\psi_\alpha(x)+b_\alpha^\dagger\varphi_\alpha(x)]\\ &=\sum_\alpha\,[a_\alpha\psi_\alpha(\boldsymbol{x})e^{-ip_\alpha^-x^+/2}+b_\alpha^\dagger\varphi_\alpha(\boldsymbol{x})e^{ip_\alpha^-x^+/2}],\end{aligned} \tag{2.5}$$

where $a_\alpha$ and $b_\alpha^\dagger$ are (anti-)nucleon annihilation operators and we define $z\equiv -x^-/2$ with $\partial^+=2\partial_-=-\partial_z$ and $(x_\perp,z)\equiv x$, which allows us to treat the minus and perpendicular coordinates on equal footing. The $\psi_\alpha$ and $\varphi_\alpha$ are coordinate space 4-component spinor solutions to the light front Dirac equation with eigenvalues $p_\alpha^-/2=M-\varepsilon_\alpha$. To simplify the analysis we will temporarily ignore electromagnetic effects, but we will include them in the final numerical results. The light front mode equations in QHD-I are obtained by minimizing the $P^-$ operator (light front Hamiltonian) with the constraint [21] that $P^+=P^-$. The result is

$$-i\partial_z\psi_\alpha^-(\boldsymbol{x})=[\boldsymbol{\alpha}_\perp\cdot(\boldsymbol{p}_\perp-g_v\overline{\boldsymbol{V}}_\perp)+\beta(M+g_s\phi)]\psi_\alpha^+(\boldsymbol{x}) \tag{2.6}$$

$$\begin{aligned}p_\alpha^-\psi_\alpha^+(\boldsymbol{x})=&[-i\partial_z+2g_v\overline{V}^-]\psi_\alpha^+(\boldsymbol{x})+[\boldsymbol{\alpha}_\perp\cdot(\boldsymbol{p}_\perp-g_v\overline{\boldsymbol{V}}_\perp)\\ &+\beta(M+g_s\phi)]\psi_\alpha^-(\boldsymbol{x}),\end{aligned} \tag{2.7}$$

with

$$\Lambda_\pm\psi_\alpha=\tfrac{1}{2}\gamma^0\gamma^\pm\psi_\alpha=\psi_\alpha^\pm, \tag{2.8}$$

$$\partial^+\overline{V}^\mu=\partial^+V^\mu-\partial^\mu V^+. \tag{2.9}$$

Using standard manipulations [20] and defining $\varepsilon_F$ as the energy of the highest occupied state, we find the Green's function to be

$$\begin{aligned}G(x,y)=&\sum_\alpha\,\psi_\alpha(\boldsymbol{x})\overline{\psi}_\alpha(\boldsymbol{y})e^{-ig_v[\Lambda(\boldsymbol{x})-\Lambda(\boldsymbol{y})]}\\ &\times\int\frac{dk^-}{2\pi}e^{-ik^-(x^+-y^+)/2}\\ &\times\left[\frac{1}{k^--p_\alpha^-+i\varepsilon}+2\pi i\,\delta(k^--p_\alpha^-)\,\theta(\varepsilon_F-\varepsilon_\alpha)\right]\\ \equiv&G^D(x,y)+G^C(x,y),\end{aligned} \tag{2.10}$$

where the superscripts $D$ and $C$ represent the disconnected and connected parts of the nucleon Green's function, respectively. The connected part is relevant to deep inelastic scattering and is given by

$$G^C(x,y)=i\sum_{\alpha\in F}\,\psi_\alpha(\boldsymbol{x})\overline{\psi}_\alpha(\boldsymbol{y})e^{-ig_v[\Lambda(\boldsymbol{x})-\Lambda(\boldsymbol{y})]}e^{-ip_\alpha^-(x^+-y^+)/2}, \tag{2.11}$$

where the sum is over occupied levels $\alpha$ in the Fermi sea $F$. We now substitute Eq. (2.11) into Eq. (2.2), first defining $(\boldsymbol{k}_\perp,k^+)\equiv\boldsymbol{k}$ where $\boldsymbol{k}\cdot\boldsymbol{x}=\boldsymbol{k}_\perp\cdot\boldsymbol{x}_\perp+k^+z=\boldsymbol{k}_\perp\cdot\boldsymbol{x}_\perp-k^+x^-/2$, $d\boldsymbol{x}=d^2\boldsymbol{x}_\perp dz$, $d\boldsymbol{k}=d^2\boldsymbol{k}_\perp dk^+$ and

$$\psi_\alpha''(\boldsymbol{k})\equiv\int d\boldsymbol{x}e^{-i\boldsymbol{k}\cdot\boldsymbol{x}}e^{-ig_v\Lambda(\boldsymbol{x})}\psi_\alpha(\boldsymbol{x}). \tag{2.12}$$

We find

$$\chi^A(k,P)=(2\pi)^2\sum_{\alpha\in F}\,\psi_\alpha''(\boldsymbol{k})\overline{\psi}_\alpha''(\boldsymbol{k})\,\delta(k^--p_\alpha^-). \tag{2.13}$$

The motivation for the ''double-prime'' notation is the subject of the following section.

### III. WAVE FUNCTION SUBTLETIES

It would be useful to express $\chi^A(k,P)$ in terms of solutions of the ordinary Dirac equation, because one may use a standard computer program [24]. If we use Eq. (2.12) we find that these ''double-primed'' fields satisfy another version of the mode equations (2.6) and (2.7) following from an application of the Soper-Yan transformation Eq. (2.4), and are given by

$$[-i\partial_z - g_v V^+]\psi''^-_\alpha(x) = [\boldsymbol{\alpha}_\perp\cdot(\boldsymbol{p}_\perp - g_v\boldsymbol{V}_\perp) + \beta(M+g_s\phi)]\psi''^+_\alpha(x) \tag{3.1}$$

$$[i\partial_z + g_v V^+ - 2g_v\overline{V^-} + p^-_\alpha]\psi''^+_\alpha(x) = [\boldsymbol{\alpha}_\perp\cdot(\boldsymbol{p}_\perp - g_v\boldsymbol{V}_\perp) + \beta(M+g_s\phi)]\psi''^-_\alpha(x). \tag{3.2}$$

If one multiplies Eq. (3.1) by $\gamma^+$ and Eq. (3.2) by $\gamma^-$ and adds the two equations, using $V^+ = V^- = \overline{V^-} = V^0$, one obtains

$$[-\gamma^3(i\partial_z + p^-_\alpha/2) + \gamma^0(p^-_\alpha/2 - g_v V^0)]\psi''_\alpha(x) = [\boldsymbol{\gamma}_\perp\cdot\boldsymbol{p}_\perp + M + g_s\phi]\psi''_\alpha(x), \tag{3.3}$$

which looks nearly like the ordinary Dirac equation with the exception of the $\gamma^3 p^-_\alpha/2$ term. To remove this term, we set

$$\tilde{\psi}_\alpha(x) \equiv e^{-ip^-_\alpha z/2}\psi''_\alpha(x) \tag{3.4}$$

and substitute into Eq. (3.3), so that

$$\gamma^0(p^-_\alpha/2 - g_v V^0)\tilde{\psi}_\alpha(x) = [\boldsymbol{\gamma}\cdot\boldsymbol{p} + M + g_s\phi]\tilde{\psi}_\alpha(x), \tag{3.5}$$

which looks superficially like the ordinary Dirac equation for the $\psi'$ fields that appear in the Lagrangian. There is a subtle difference; since the light front energy is given by $k^2 = (\boldsymbol{k}_\perp^2 + M^2)/k^+$, Eq. (3.3) has support for $k^+ > 0$. This means Eq. (3.5) has support for $k^3 > -p^-_\alpha/2$ which in turn implies that it can only be considered the ordinary Dirac equation with a momentum cutoff at $p^-_\alpha/2 \simeq M$. This restriction is nearly superfluous since the probability that a nucleon is carrying $|k^3| > M$ is suppressed by a factor of order $e^{-M^2R^2}$ with $R$ being the nuclear radius. This allows us to effectively identify $\tilde{\psi}_\alpha \simeq \psi'$ which gives the approximate relationships among the (equal time) Lagrangian fields $\psi'$, the Soper-Yan transformed light front fields $\psi$, and the untransformed light front fields $\psi''$ that appear in Eq. (2.13). We have

$$\psi'_\alpha(x) \simeq e^{-ip^-_\alpha z/2}\psi''_\alpha(x) \tag{3.6}$$

$$= e^{-ip^-_\alpha z/2}e^{-ig_v\Lambda(x)}\psi_\alpha(x). \tag{3.7}$$

Equation (3.7) is the approximate relationship between the $\psi$ and $\psi'$ fields in Ref. [21]. We now are ready to derive a representation of Eq. (2.1) in terms of these nucleon wave functions.

### IV. DERIVATION OF THE PLUS MOMENTUM DISTRIBUTION

In Ref. [21], it was determined that a plus momentum distribution in QHD-I is given by

$$f(k^+) = 2\sum_{\alpha\in F}\int d^2\boldsymbol{x}_\perp |\psi^+_\alpha(\boldsymbol{x}_\perp, k^+)|^2. \tag{4.1}$$

This distribution peaks at $k^+/\overline{M} \equiv y \simeq 0.8$ for $^{16}$O, (with smaller values for heavier nuclei) but is not the distribution obtained from the covariant formalism of Sec. II. The connection between this $f(y)$ and the covariant $f_N(y)$ was made in Ref. [16]; it was determined that, in the limit of infinite nuclear matter, the relationship between $f(y)$ and $f_N(y)$ is simply a shift in the argument by the vector meson potential,

$$f(y) = f_N(y + g_v V^+/\overline{M}). \tag{4.2}$$

This shift arises from the use of the Soper-Yan transformation Eq. (2.4) where the $\psi'$ fields are those appearing in the Lagrangian and are used to determine $f_N(y)$, whereas the $\psi$ fields are used to determine $f(y)$. In finite nuclei, this relationship is somewhat more complicated since the vector meson potential is no longer a constant over all space. We start with Eq. (2.13), and see that

$$\mathrm{Tr}\,\gamma^+\chi^A(k,P) = (2\pi)^2\sum_{\alpha\in F}\mathrm{Tr}[\gamma^+\psi''_\alpha(\boldsymbol{k})\overline{\psi''_\alpha}(\boldsymbol{k})]\delta(k^- - p^-_\alpha)$$

$$= 8\pi^2\sum_{\alpha\in F}|\psi''^+_\alpha(\boldsymbol{k})|^2\delta(k^- - p^-_\alpha).$$

Substituting into Eq. (2.1) we obtain

$$f_N(y) = \frac{2}{(2\pi)^2}\sum_{\alpha\in F}\int d\boldsymbol{k}\,\delta(y - k^+/\overline{M})|\psi''^+_\alpha(\boldsymbol{k})|^2. \tag{4.3}$$

Use of Parseval's identity and integrating over $k^+$ gives us our main result:

$$f_N(y) = 2\overline{M}\sum_{\alpha\in F}\int d^2\boldsymbol{x}_\perp |\psi''^+_\alpha(\boldsymbol{x}_\perp, \overline{M}y)|^2, \tag{4.4}$$

so the plus momentum distribution is related to Fourier transform of the $\psi''$ wave functions. One can see the similarity to Eq. (4.1); the difference lies entirely in Eq. (2.12). It should be emphasized that this result does not depend on the approximation in Sec. III.

We shall use $f_N(y)$ to compute the nuclear structure function $F_{2A}(x)$ in Sec. V, but first we derive a version of the Hugenholtz–van Hove theorem valid for finite nuclei. To do that, multiply Eq. (4.3) by $y$ and integrate,

$$\langle y\rangle \equiv \int dy y f_N(y) = \frac{2}{(2\pi)^2} \sum_{\alpha\in F} \int d\boldsymbol{k} \frac{k^+}{\overline{M}} |\psi''^+_\alpha(\boldsymbol{k})|^2. \tag{4.5}$$

Now remove the plus projections and reexpress $\psi''$ and its complex conjugate in coordinate spaces $\boldsymbol{x}$ and $\boldsymbol{x}'$. One can then integrate over $\boldsymbol{k}$ yielding a delta function $\delta(\boldsymbol{x}-\boldsymbol{x}')$ that allows integration over $\boldsymbol{x}'$ yielding

$$\langle y\rangle = \frac{1}{\overline{M}} \sum_{\alpha\in F} \int d\boldsymbol{x} \psi''^\dagger_\alpha(\boldsymbol{x}) \gamma^0\gamma^+ i\partial^+ \psi''_\alpha(\boldsymbol{x}).$$

We wish to look at the $\psi$ fields in order to understand our result in the context of Ref. [21], so we need to perform the Soper-Yan transformation Eq. (2.4) and use $X^\dagger\gamma^0 \equiv \overline{X}$

$$\langle y\rangle = \frac{1}{\overline{M}} \sum_{\alpha\in F} \int d\boldsymbol{x} \overline{\psi}_\alpha(\boldsymbol{x}) \gamma^+ [i\partial^+ + g_v V^+(\boldsymbol{x})] \psi_\alpha(\boldsymbol{x}).$$

If we explicitly put in the the nuclear state vectors, we can perform the sum on $\alpha$ by inserting creation and annihilation operators; we can add the time dependence for free since it is unaffected by $\partial^+$ and cancels with both fermion fields, and the vector potential is static. We have effectively undone the substitution Eq. (2.5) and now have an expectation value of an operator

$$\langle y\rangle = \frac{1}{M_A} \int d\boldsymbol{x} \langle \overline{\psi}\gamma^+ [i\partial^+ + g_v V^+]\psi\rangle. \tag{4.6}$$

The second term of Eq. (4.6) was essentially included by Birse [25] via a kinematic argument; here it follows from a fully covariant light front treatment. Using the vector meson field equation in QHD-I

$$\partial_\mu V^{\mu+} + m_v^2 V^+ = g_v \overline{\psi}\gamma^+ \psi,$$

integrating by parts, and antisymmetrizing one can re-express the second term of Eq. (4.6) as

$$\begin{aligned}\langle y\rangle &= \frac{1}{M_A} \int d\boldsymbol{x} \langle \overline{\psi}\gamma^+ i\partial^+\psi + m_v^2 V^+ V^+ + V^{+\mu} V^+_\mu\rangle \\ &= \frac{1}{M_A} \int d\boldsymbol{x} \langle T^{++} - \partial^+\phi\partial^+\phi\rangle \\ &= \frac{1}{M_A}(P^+ - P_s^+) = 1 - \frac{P_s^+}{M_A} \simeq 1,\end{aligned} \tag{4.7}$$

where $T^{++}$ is one component of the canonical energy momentum tensor, $P_s^+$ is the plus momentum of the scalar meson fields, and $P^+$ is the total nuclear plus momentum. The result Eq. (4.7) constitutes an analog of the Hugenholtz–van Hove theorem [17] for finite systems; the equality becomes exact in the nuclear matter limit, where the scalar meson contribution vanishes, as shown in our previous work [16]. This means that we may anticipate that the binding effect will again be small. The vector operator ''mixing'' and the scalar meson contribution will be elaborated on in a more general context in Sec. VI.

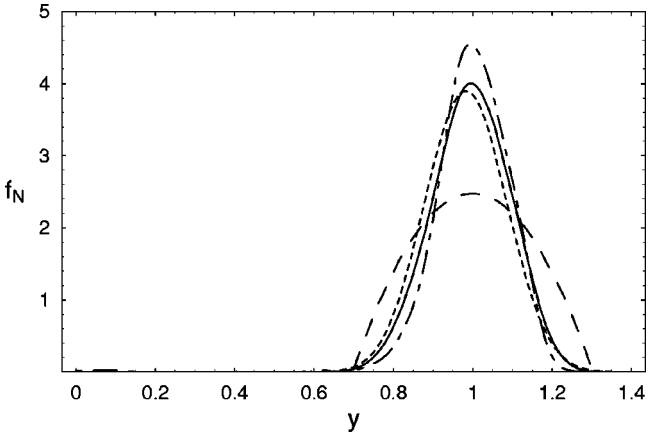


FIG. 2. Plus momentum distributions, $f_N(y)$, for $^{40}$Ca (solid), $^{16}$O (short dashes), $^{208}$Pb (dot-dashes), and nuclear matter (long dashes).

It is also worthwhile to explicitly evaluate the expression (4.4) for $f_N(y)$ in the limit of infinite nuclear matter. In this case, $V^0 = V^+ = V^-$ are constant and $\boldsymbol{V}_\perp = 0$, so we find

$$\Lambda(z,\boldsymbol{x}_\perp) = \int_z^\infty dz' V^0(z',\boldsymbol{x}_\perp) = -V^0 z = -V^+ z, \tag{4.8}$$

so that Eq. (2.12) becomes

$$\begin{aligned}\psi''^+_\alpha(\boldsymbol{k}) &= \int d\boldsymbol{x} e^{-i\boldsymbol{k}_\perp\cdot\boldsymbol{x}_\perp} e^{-i(k^+ - g_v V^+)z} \psi^+_\alpha(\boldsymbol{x}) \\ &= \psi^+_\alpha(\boldsymbol{k}_\perp, k^+ - g_v V^+).\end{aligned} \tag{4.9}$$

Therefore Eq. (4.4) becomes

$$f_N(y) = 2\overline{M} \sum_{\alpha\in F} \int d^2\boldsymbol{x}_\perp |\psi^+_\alpha(\boldsymbol{x}_\perp, \overline{M}y - g_v V^+)|^2, \tag{4.10}$$

which is simply the expression (4.1) modified by a shift in the argument of $g_v V^+/\overline{M}$. Thus we find Eq. (4.2) is satisfied in the nuclear matter limit. It is important to stress that all that is recovered here is the shift in the argument and not any particular form of the plus momentum distribution that arises from the specific model used.

## V. NUCLEAR STRUCTURE FUNCTIONS

We determine the wave functions appearing in Eq. (4.4) numerically from a relativistic self-consistent treatment following Horowitz and Serot [26] using the same program [24] that includes electromagnetic effects. The plus momentum distribution follows and is given in Fig. 2 for $^{16}$O, $^{40}$Ca, $^{208}$Pb and in the nuclear matter limit (the $^{16}$O calculation is also shown in Fig. 4). One can see that the peaks appear near $y=1$ as required by the Hugenholtz–van Hove theorem Eq. (4.7).

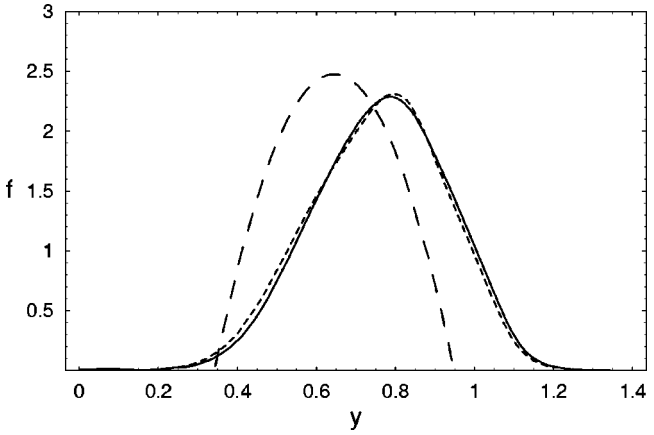


FIG. 3. $f(y)$ distributions for $^{16}$O (solid) and nuclear matter (long dashes) after application of the Soper-Yan transformation along with the $^{16}$O distribution from Ref. [21] (short dashes). Note that the peaks occur at $y<1$.

It is worth noting that application of the Soper-Yan transformation Eq. (2.4) to the $\psi''$ wave functions obtained from the equal time wave functions reproduces the plus momentum distributions, including the correct asymmetry, of the light front calculations in Ref. [21], which did not use the approximation (3.6). We show the comparison of our oxygen calculation to that of Ref. [21] in Fig. 3; the agreement of these two curves demonstrates the excellence of the approximation relating the light front and equal time wave functions. One can see that the effect in finite nuclei of the Soper-Yan transformation is to shift and broaden the plus momentum distribution, while in nuclear matter (also shown in Fig. 3) it is just a shift. If these distributions were to be used in the nuclear structure function Eq. (5.2) though, since $\langle y\rangle \simeq 0.8$ for oxygen, the ratio function [Eq. (5.4) discussed later] would fall precipitously to nearly zero at $x\simeq 0.6$ in stark contradiction with experiment.

We also evaluated the plus momentum distribution Eq. (4.4) with the simple nonrelativistic harmonic oscillator shell model as an additional check on our method. These (equal time) wave functions give us an explicit, although approximate in the sense of Sec. III, closed form of the plus momentum distribution for $^{16}$O:

$$f_N(y)\simeq \frac{\xi}{\sqrt{16\pi}}[e^{-\xi^2(\eta_{1s}-y)^2} + 2\{1+\xi^2(\eta_{1p}-y)^2\}e^{-\xi^2(\eta_{1p}-y)^2}], \quad (5.1)$$

with $\eta_{nl}=M+\omega(2(n-1)+l+3/2)-v_0$ where $v_0 \simeq 50$ MeV, and $\xi\equiv \bar{M}b$ where $b=(m\omega)^{-1/2}\simeq 1.6$ fm is the oscillator length that is fit to the root mean square radius of oxygen $\langle R^2\rangle^{1/2}\simeq 2.7$ fm. The distribution Eq. (5.1) narrows for larger $\xi$ that corresponds to an increasing root mean square radius. This distribution is plotted in Fig. 4 where one can see that it peaks near $y=1$ like the relativistic Hartree calculation, but appears to have a smaller value of $\langle y\rangle$. It is worth noting that the Hartree calculations are in the relativistic equal time framework and put into our relativistic light front formalism, while the harmonic oscillator calculations are nonrelativistic and put into our relativistic formalism.

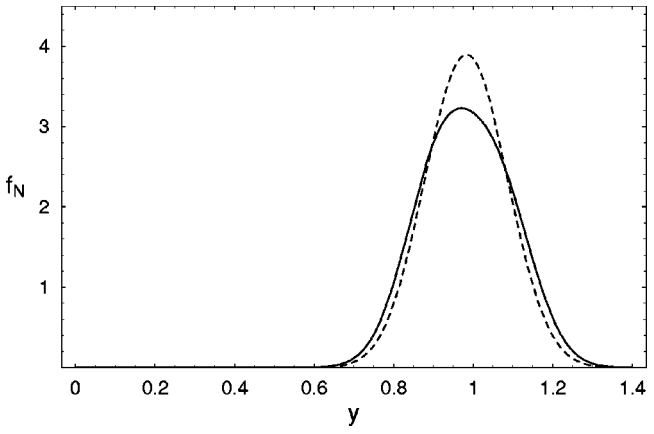


FIG. 4. Plus momentum distribution for $^{16}$O calculated with harmonic oscillator (solid curve) and relativistic Hartree (dashed curve) wave functions.

The structure function is given by the convolution

$$\frac{F_{2A}(x_A)}{A}=\int_{x_A}^{A} dy f_N(y) F_{2N}(x_A/y), \quad (5.2)$$

with $x_A\equiv Q^2A/2P\cdot q = xM/\bar{M}$. The assumption that nuclear effects do not modify the structure of the nucleon is embodied in Eq. (5.2) by the use of the structure function of a free nucleon; we use the parametrization [27]

$$F_{2N}(x)=0.58\sqrt{x}(1-x)^{2.8}+0.33\sqrt{x}(1-x)^{3.8}+0.49(1-x)^8. \quad (5.3)$$

The experiments measure the ratio function, defined as

$$R(x)=\frac{F_{2A}(x_A)}{AF_{2N}(x)}. \quad (5.4)$$

The results of our calculations are plotted for $^{16}$O, $^{40}$Ca, $^{208}$Pb and in the nuclear matter limit in Fig. 5 showing data for carbon, calcium, and gold from SLAC-E139 [28] and an extrapolation [29] for the nuclear matter calculation. The most striking result is that these calculations fail to reproduce the EMC effect; the curves consistently miss the minima in the data, and the agreement gets worse with increasing $A$. Another important result is that the ratio function does not fall to zero as would be the case if the small effective mass ($\sim 0.56M$ for nuclear matter in QHD-I) were the relevant parameter describing the binding effect that would follow from using Eq. (4.1) instead of Eq. (4.4). The results also show a minimum near $x\simeq 0.6$ for oxygen and nuclear matter that is deeper than the calcium and lead calculations. This is a curious feature that contradicts the trend in experimental data, and is due to the effects of two parameters.

The first, and most important, is that of the location of the peak of the plus momentum distribution given by Eq. (4.7), which gradually approaches $y=1$ as the nuclear matter limit is reached. This is due to the fact that scalar mesons carry a small amount of plus momentum [21] that vanishes as $A$

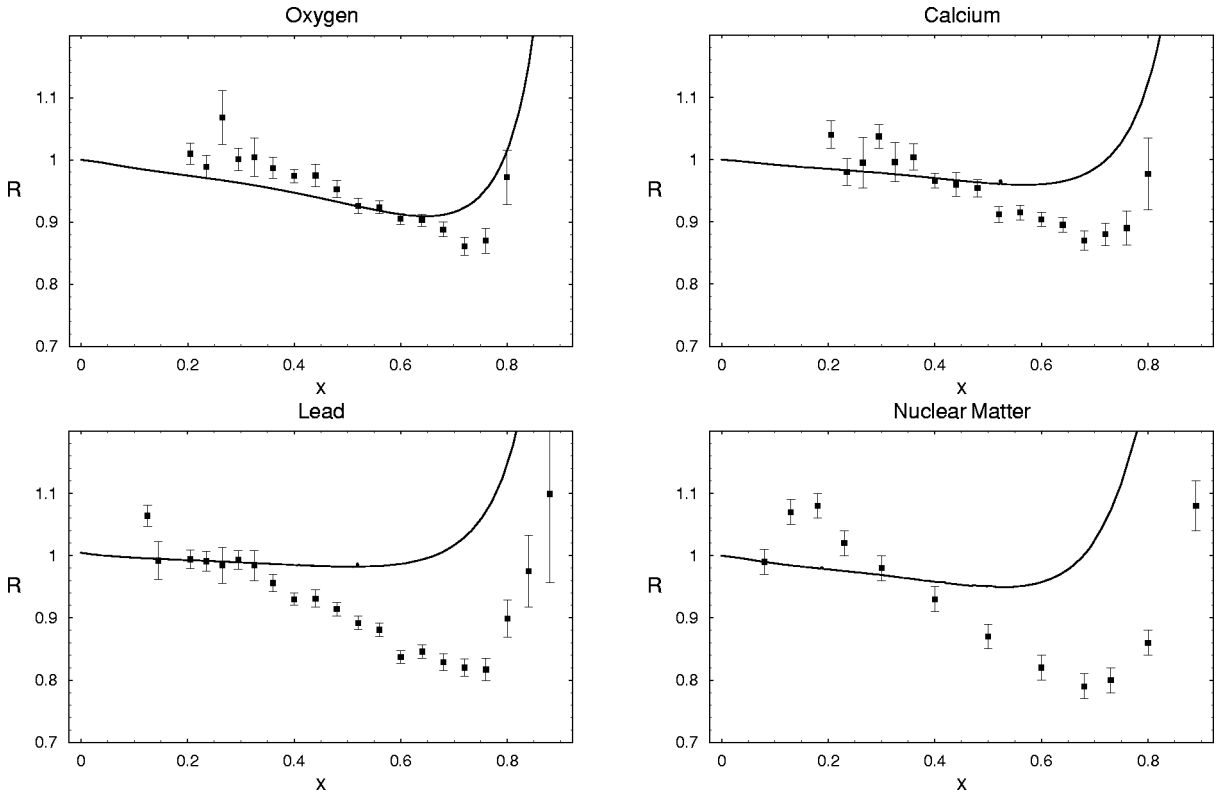


FIG. 5. Ratio functions for $^{16}$O, $^{40}$Ca and $^{208}$Pb showing data for carbon, calcium and gold, respectively, from SLAC-E139 [28]. The nuclear matter calculation shows extrapolated data [29].

$\rightarrow\infty$. The closer to $y=1$ the peak is in Fig. 2, the less pronounced the minimum in Fig. 5 will be all else remaining constant. The second effect is due to $\bar{M}$, which reaches a minimum at $^{56}$Fe corresponding to a more pronounced minimum of the ratio function than for $A<56$ or $A>56$, keeping the scalar meson contribution constant.

Using a Gaussian parametrization of the plus momentum distribution and the experimental binding energy per nucleon via the semiempirical mass formula, we have modeled the dependence of the minimum of the ratio function, $R(x \simeq 0.72)$, on the number of nucleons in the nucleus in Fig. 6.

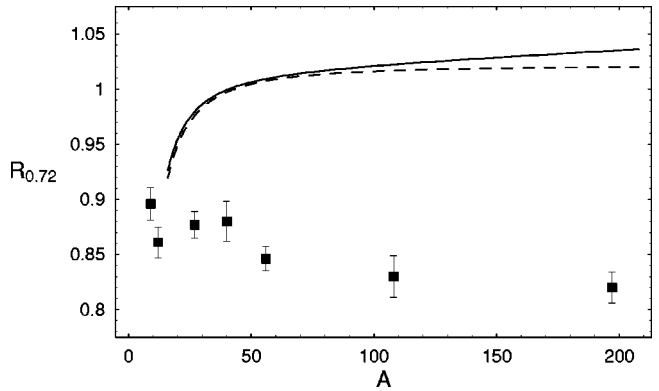


FIG. 6. $R(x=0.72)$ as a function of $A$ including scalar meson and binding effects (solid line), and leaving binding energy per nucleon constant at $-8.5$ MeV (dashed line). The data are from SLAC-E139 [28].

The motivation for the use of Gaussian plus momentum distributions is based on the expansion [5]

$$F_{2A}(x_A)=F_{2N}(x_A)+\epsilon x_A F'_{2N}(x_A) + \gamma[2x_A F'_{2N}(x_A)+x_A^2 F''_{2N}(x_A)], \quad (5.5)$$

where

$$\epsilon \equiv 1-\int dy y f_N(y) \quad (5.6)$$

$$\gamma \equiv \int dy (y-1)^2 f_N(y). \quad (5.7)$$

The Gaussian parametrization uses the peak location and width, $\langle y\rangle$ and $(\langle y^2\rangle-\langle y\rangle^2)^{1/2}$, respectively, from the relativistic Hartree calculations in Fig. 2, and is normalized to unity. This allows us to obtain a plus momentum distribution for any $A$ with minimal effort. We show the combined effect of scalar mesons and binding energy per nucleon on the ratio function along with the effect of scalar mesons alone using a constant binding energy per nucleon of $-8.5$ MeV independent of $A$. It can be seen that a changing $\bar{M}$ with $A$ has the most effect for nuclei much larger than iron, but does not change the general trend that the minimum of the ratio function becomes less pronounced as $A$ increases due to the vanishing scalar meson contribution and the peak of the plus momentum distribution approaching unity. This dependence of the binding effect on $A$ is quite different, both in magni-

tude and shape, than the trend in experimental data summarized in Ref. [29], which satisfies $R(x\simeq 0.72)\sim A^{-1/3}$, so that the minimum becomes more pronounced as $A$ increases. This fully demonstrates the inadequacy of conventional nucleon-meson dynamics to explain the EMC effect.

## VI. SCALAR MESON CONTRIBUTION TO PLUS MOMENTUM AND MORE GENERAL CONSIDERATIONS

The average value of $y$, given by Eq. (4.7), yields the nucleon contribution to the plus momentum, and is less than 1, which can be seen in Fig. 2. We now address the remaining plus momentum in finite nuclei. Previous results [21] show that a small fraction ($\delta y\sim 0.005$) of the plus momentum is carried by the scalar mesons, which vanishes as the nuclear matter limit is approached. This is due to the fact that scalar mesons couple to gradients in the scalar density (arising mainly from the surface of finite nuclei), which vanish as $A\rightarrow\infty$. The question is: why are scalar mesons allowed to carry plus momentum and not vector mesons?

The simplest answer lies in the Dirac structure of Eq. (2.1); the $\gamma^+$ in the trace picks out terms in the full interacting Green's function with an odd number of $\gamma$ matrices, which includes all Lorentz vector interactions and excludes Lorentz scalar interactions. The Dirac structure of $f_N(y)$ is directly related to the Dirac structure of the energy momentum tensor, so the answer also lies there and illuminates a problem with conventional nucleon-meson dynamics. The component of the energy momentum tensor relevant to the plus momentum, from a chiral Lagrangian containing isoscalar vector mesons, scalar mesons and pions, is given by [30,31]

$$T^{++}=V^{+\mu}V^{+}_{\mu}+m_v^2V^+V^++\bar{\psi}\gamma^+i\partial^+\psi+\partial^+\phi\partial^+\phi+\partial^+\boldsymbol{\pi}\cdot\partial^+\boldsymbol{\pi}+\boldsymbol{\pi}\cdot\partial^+\boldsymbol{\pi}\frac{\boldsymbol{\pi}\cdot\partial^+\boldsymbol{\pi}}{\pi^2}\left(1-\frac{f^2}{\pi^2}\sin^2\frac{\pi}{f}\right). \tag{6.1}$$

Since each of the terms in Eq. (6.1) involves one of the fields, it is natural to associate each term with a particular contribution to the plus momentum. This decomposition, though, is not well defined; field equations relate various components. We see the first three terms of Eq. (6.1) appear in $\langle y\rangle$, which defines the nucleon contribution to the total nuclear plus momentum, in the derivation of the Hugenholtz–van Hove theorem Eq. (4.7); we are not allowed to have the vector mesons contribute a well defined fraction of plus momentum. This means that one could trade certain mesonic degrees of freedom for nucleons by replacing mesonic vertices with nucleon point couplings, for example, in line with the general concept of effective field theory. In our case the first three terms are related by the vector meson field equation, but the fourth is left out since the scalar mesons couple to the scalar density $\bar{\psi}\psi$, which is not present in Eq. (6.1). Therefore the scalar mesons (and pions) contribute a well defined fraction of plus momentum. These explicit meson contributions create an EMC binding effect, but the pionic contributions are also limited by nuclear Drell-Yan experiments [32] to carrying about 2% of the plus momentum, which is insufficient to account for the entire EMC effect that corresponds to about 5% of the plus momentum for iron.

## VII. SUMMARY AND DISCUSSION

The depth of the minimum in the EMC effect is known to have a monotonically increasing behavior with $A$, which has been studied in Refs. [28,29] among others. Our present theory is defined by the use of the mean-field approximation, along with the assumption that nuclear effects do not modify the structure of the nucleon. This theory leads to results in severe disagreement with experiment. Not only do we find that the depth of the minimum is monotonically decreasing with $A$, but it has a smaller magnitude than experiment. These results, which fail to capture any of the important features of the experiments, represent a failure of relativistic mean field theory. Furthermore, the plus momentum distributions we compute give $\langle y\rangle\simeq 1$, which indicates that nearly all of the plus momentum is carried by the nucleons. In order to reproduce the data, the nucleon plus momentum must be decreased by some mechanism that becomes more important at larger $A$. Nucleon-nucleon correlations cannot take plus momentum from nucleons, and explicit mesonic components in the nuclear Fock state wave function carrying plus momentum are limited [33–35] by Drell-Yan experiments [32]. Thus it appears that the EMC effect may be due to something outside of conventional nucleon-meson dynamics. For example, true modifications to nucleon structure caused by nuclear interactions could be important, in which case one would need to use models such as the mini-delocalization model [5], quark-meson coupling model [36–38] or the chiral quark soliton model reviewed in [39] to include those effects.

## ACKNOWLEDGMENT

We would like to thank the U.S. DOE for partial support of this work.

[1] J. J. Aubert *et al.*, European Muon Collaboration, Phys. Lett. **123B**, 275 (1983).
[2] M. Arneodo, Phys. Rep. **240**, 301 (1994).
[3] D. F. Geesaman, K. Saito, and A. W. Thomas, Annu. Rev. Nucl. Part. Sci. **45**, 337 (1995).
[4] G. Piller and W. Weise, Phys. Rep. **330**, 1 (2000).
[5] L. L. Frankfurt and M. I. Strikman, Phys. Rep. **160**, 235 (1988).
[6] G. A. Miller, Prog. Part. Nucl. Phys. **45**, 83 (2000).
[7] S. J. Brodsky, H. C. Pauli, and S. S. Pinsky, Phys. Rep. **301**, 299 (1998).
[8] *Theory of Hadrons and Light-Front QCD*, edited by S. D.

Glazek (World Scientific, Singapore, 1994).
[9] M. Burkardt, Adv. Nucl. Phys. **23**, 1 (1993).
[10] S. J. Brodsky and G. P. Lepage, in *Perturbative Quantum Chromodynamics*, edited by A. Mueller (World Scientific, Singapore, 1989).
[11] X.-D. Ji, Comments Nucl. Part. Phys. **21**, 123 (1992).
[12] W.-M. Zhang, Chin. J. Phys. (Taipei) **32**, 717 (1994).
[13] R. J. Perry, in *Hadron Physics 94*, Topics on the Structure and Interactions of Hadronic Systems, edited by V. E. Herscovitz *et al*. (World Scientific, Singapore, 1994).
[14] A. Harindranath, in *Light-Front Quantization and Non-Perturbative QCD*, edited by J.P. Vary and F. Wölz (International Institute of Theoretical and Applied Physics, Ames, 1997).
[15] J. R. Cooke and G. A. Miller, nucl-th/0112037.
[16] G. A. Miller and J. R. Smith, Phys. Rev. C **65**, 015211 (2002).
[17] N. M. Hugenholtz and L. van Hove, Physica (Amsterdam) **24**, 363 (1958).
[18] H. Jung and G. A. Miller, Phys. Lett. B **200**, 351 (1988).
[19] B. D. Serot and J. D. Walecka, Int. J. Mod. Phys. E **6**, 515 (1997).
[20] B. D. Serot and J. D. Walecka, Adv. Nucl. Phys. **16**, 1 (1986).
[21] P. G. Blunden, M. Burkardt, and G. A. Miller, Phys. Rev. C **60**, 055211 (1999).
[22] D. E. Soper, Phys. Rev. D **4**, 1620 (1971).
[23] T.-M. Yan, Phys. Rev. D **7**, 1760 (1973).
[24] C. J. Horowitz, in *Nuclear Structure*, Computational Nuclear Physics Vol. 1, edited by K. Langanke, J. A. Maruhn, and S. E. Koonin (Springer-Verlag, New York, 1991).
[25] M. C. Birse, Phys. Lett. B **299**, 186 (1993).
[26] C. J. Horowitz and B. D. Serot, Nucl. Phys. **A368**, 503 (1981).
[27] J. G. de Groot *et al.*, Phys. Lett. **82B**, 456 (1979).
[28] J. Gomez *et al.*, SLAC-E139, Phys. Rev. D **49**, 4348 (1994).
[29] I. Sick and D. Day, Phys. Lett. B **274**, 16 (1992).
[30] G. A. Miller, Phys. Rev. C **56**, 2789 (1997).
[31] G. A. Miller and R. Machleidt, Phys. Rev. C **60**, 035202 (1999).
[32] D. M. Alde *et al.*, Phys. Rev. Lett. **64**, 2479 (1990).
[33] R. P. Bickerstaff, M. C. Birse, and G. A. Miller, Phys. Rev. Lett. **53**, 2532 (1984).
[34] M. Ericson and A. W. Thomas, Phys. Lett. **148B**, 191 (1984).
[35] E. L. Berger, Nucl. Phys. **B267**, 231 (1986).
[36] K. Saito and A. W. Thomas, Phys. Lett. B **327**, 9 (1994).
[37] O. Benhar, V. R. Pandharipande, and I. Sick, Phys. Lett. B **469**, 19 (1999).
[38] F. Gross and S. Liuti, Phys. Rev. C **45**, 1374 (1992).
[39] D. Diakonov and V. Y. Petrov, hep-ph/0009006.